RELAXATION PHENOMENA IN CLASSICAL AND QUANTUM SYSTEMS*

B. Spagnolo[a†], P. Caldara[a], A. La Cognata[a], G. Augello[a]
D. Valenti[a], A. Fiasconaro[b], A.A. Dubkov[c], G. Falci[d]

[a]Dipartimento di Fisica, Group of Interdisciplinary Physics
Università di Palermo and CNISM
Viale delle Scienze, edificio 18, 90128 Palermo, Italy
[b]Departamento de Física de la Materia Condensada
ICMA (CSIC — Universidad de Zaragoza), 50009 Zaragoza, Spain
[c]Radiophysics Department, Nizhny Novgorod State University
23 Gagarin Avenue, 603950 Nizhny Novgorod, Russia
[d]Dipartimento di Fisica e Astronomia, Università di Catania
Via Santa Sofia, 64, 95123 Catania, Italy

(Received April 23, 2012)

Version corrected according to Erratum, Acta Phys. Pol. B **47**, 1179 (2016)

Relaxation phenomena in three different classical and quantum systems are investigated. First, the role of multiplicative and additive noise in a classical metastable system is analyzed. The mean lifetime of the metastable state shows a nonmonotonic behavior with a maximum as a function of both the additive and multiplicative noise intensities. In the second system, the simultaneous action of thermal and non-Gaussian noise on the dynamics of an overdamped point Josephson junction is studied. The effect of a Lévy noise generated by a Cauchy–Lorentz distribution on the mean lifetime of the superconductive metastable state, in the presence of a periodic driving, is investigated. We find resonant activation and noise enhanced stability in the presence of Lévy noise. Finally, the time evolution of a quantum particle moving in a metastable potential and interacting with a thermal reservoir is analyzed. Within the Caldeira–Legget model and the Feynman–Vernon functional approach, we obtain the time evolution of the population distributions in the position eigenstates of the particle, for different values of the thermal bath coupling strength.

DOI:10.5506/APhysPolB.43.1169
PACS numbers: 05.10.Gg, 05.40.–a, 74.50.+r, 42.50.Lc

* Presented at the XXIV Marian Smoluchowski Symposium on Statistical Physics, "Insights into Stochastic Nonequilibrium", Zakopane, Poland, September 17–22, 2011.

† bernardo.spagnolo@unipa.it

1. Introduction

In this work, we will consider the transient dynamics of three different classical and quantum systems, namely: *(i)* a classical metastable model system, *(ii)* an overdamped Josephson junction, and *(iii)* a quantum metastable system. *(i)* The dynamics of an asymmetric bistable system in the presence of additive and multiplicative noise sources is investigated. The role of both noise sources on the mean escape time from the metastable state is studied. We find a nonmonotonic behavior with a maximum of the mean escape time as a function of both noise intensities, revealing the presence of the noise enhanced stability effect [1–18]. *(ii)* The influence of non-Gaussian noise on the transient dynamics of a short overdamped Josephson junction, in the framework of the resistively shunted junction model and in the presence of a periodic driving, is investigated. The mean lifetime of the superconductive metastable state of the Josephson junction, namely the mean switching time, as a function of the frequency of the driving current signal and the noise intensity is studied. Resonant activation [19–22] and noise enhanced stability phenomena, in the presence of a Cauchy–Lorentz Lévy noise and thermal noise sources, are observed in the range of parameter values investigated. *(iii)* In the third system, the dynamics of a quantum particle moving in a metastable potential and interacting with an environmental thermal noise is analyzed. Within the framework of the Caldeira–Leggett model, by using the Feynman–Vernon functional approach in discrete variable representation [23], we obtain the time evolution of the population distributions in the position eigenstates of the particle, for different values of the thermal bath coupling strength.

2. Metastable model system with additive and multiplicative noise

The interaction of a classical system with its environment, which is always noisy, is usually modeled by noise source terms in the dynamical equation of the system. The resulting stochastic differential equation contains, in general, additive and multiplicative noise terms. This last noise source is characterized by an amplitude which is a function of the order parameter of the macroscopic system investigated. The role of combined multiplicative and additive noise on the dynamical behavior of the system has been investigated in many physical, biological and chemical systems [24–29]. Moreover, stochastic differential equations with multiplicative noise are ubiquitous in modeling natural science phenomena. Examples range from nonlinear quantum optics, autocatalytic chemical reactions to population dynamics and noise-induced phase transitions studies [24, 30–41]. The nonlinear interplay

between additive thermal fluctuations and multiplicative noise has been analyzed in Ref. [42].

In this work, we investigate the average escape time of an overdamped Brownian particle from a metastable state. The enhancement of stability of the metastable state is observed in the presence of both the additive and multiplicative noise. We calculate the stationary probability density function (PDF) by functional analysis technique.

2.1. The model

The stochastic differential equation useful to describe the transient dynamics of out of equilibrium systems is given by the following Langevin equation

$$\frac{dx(t)}{dt} = f(x(t)) + g(x(t))\xi(t)\,, \tag{1}$$

where $f(x(t))$ and $g(x(t))$ are arbitrary deterministic functions of the order parameter $x(t)$ and $\xi(t)$ is a Gaussian white noise with the usual statistical properties $\langle\xi(t)\rangle = 0$ and correlation function $\langle\xi(t)\xi(t+\tau)\rangle = 2\mathcal{D}\delta(\tau)$. We start from the following relation for the PDF

$$P(x,t) = \int_{-\infty}^{+\infty} dx(t)P(x(t))\delta(x - x(t)) = \langle\delta(x - x(t))\rangle\,. \tag{2}$$

The derivative of the probability density function is

$$\frac{\partial P(x,t)}{\partial t} = \frac{\partial}{\partial t}\langle\delta(x - x(t))\rangle = \frac{\partial}{\partial x}\langle\delta(x - x(t))[-\dot{x}(t)]\rangle\,. \tag{3}$$

Using Eq. (1) we obtain

$$\frac{\partial P(x,t)}{\partial t} = -\frac{\partial}{\partial x}f(x)\langle\delta(x - x(t))\rangle - \frac{\partial}{\partial x}g(x)\langle\delta(x - x(t))\xi(t)\rangle\,. \tag{4}$$

Now we use the functional analysis technique. To split the correlation formula in the second right term of Eq. (4) we use the Furutsu–Novikov formula [43]

$$\langle\mathcal{F}(t)\delta(x - x(t))\rangle = \mathcal{D}\left\langle\frac{\delta}{\delta\mathcal{F}(t)}\delta(x - x(t))\right\rangle\,, \tag{5}$$

where $\frac{\delta}{\delta\mathcal{F}(t)}$ is the operator of the functional derivative of the functional $\mathcal{F}(t)$ with respect to the generic functional $\mathcal{F}(t)$. The functional chain rule gives

$$\frac{\delta}{\delta\mathcal{F}(t)}\delta(x - x(t)) = \frac{\partial\delta(x - x(t))}{\partial x(t)}\left[-\frac{\delta x(t)}{\delta\mathcal{F}(t')}\right]\,. \tag{6}$$

In order to evaluate the last functional derivative, we formally integrate Eq. (1)

$$x(t) = \int_0^t [f(x(\tau)) + g(x(\tau))\xi(\tau))]\, d\tau \tag{7}$$

and then

$$\frac{\delta x(t)}{\delta \xi(t')} = \int_0^t d\tau \left[\frac{\delta f(x(\tau))}{\delta \xi(t')} + \frac{\delta}{\delta \xi(t')} \left(g(x(\tau))\xi(\tau) \right) \right] . \tag{8}$$

Since the functional derivative of a function is the usual derivative, we obtain

$$\frac{\delta x(t)}{\delta \xi(t')} = \int_0^t \left[\frac{\partial f(x)}{\partial x} \frac{\delta x(\tau)}{\delta \xi(t')} + \frac{\partial g(x)}{\partial x} \frac{\delta x(\tau)}{\delta \xi(t')} \xi(t) + g(x) \frac{\delta \xi(\tau)}{\delta \xi(t')} \right] d\tau . \tag{9}$$

For Gaussian noise we have $\mathcal{F}[\xi(t)] = \xi(t)$. The integration of the first and second term of Eq. (9), because of the causality principle, gives zero. The third term gives

$$\int_0^t g(x(\tau)) \frac{\delta \xi(\tau)}{\delta \xi(t')} d\tau = \int_0^t g(x(\tau)) \delta(\tau - t') d\tau = g(x(t)) . \tag{10}$$

With these results Eq. (6) becomes

$$\left\langle \delta(x - x(t))\xi(t') \right\rangle = -\mathcal{D} \frac{\partial}{\partial x} \left[\left\langle \delta(x - x(t)) \right\rangle g(x) \right] . \tag{11}$$

Therefore, from Eq. (4) we obtain the general Fokker–Planck equation for arbitrary deterministic functions $f(x)$ and $g(x)$. Then, in the case of a Gaussian white noise, the Fokker–Planck equation is

$$\frac{\partial P(x,t)}{\partial t} = -\frac{\partial}{\partial x} \left[f(x) P(x,t) \right] + \mathcal{D} \frac{\partial}{\partial x} \left[g(x) \frac{\partial}{\partial x} \left[g(x) P(x,t) \right] \right] . \tag{12}$$

Since we obtained this equation using the usual rules of ordinary calculus, this is the "Stratonovich form" of the Fokker–Planck equation [44, 45]. By equating to zero the time derivative of the PDF, we obtain the asymptotic stationary PDF

$$P_{\mathrm{st}}(x) = \mathcal{N} \exp \left(\int \frac{f(x')}{\mathcal{D} g^2(x')} dx - \ln(g(x)) \right) = \mathcal{N} e^{-\frac{V_{\mathrm{eff}}(x)}{D}} , \tag{13}$$

where $\mathcal{N}$ is the normalization constant, $f(x) = -dV(x)/dx$ is the driving force and $V_{\mathrm{eff}}(x)$ is the effective or "probabilistic" potential [31].

We choose the following function $g(x) = \sqrt{D + \mu x^2}$, with D the additive thermal noise intensity and μ the intensity of the multiplicative noise. For our metastable model system we use a quartic asymmetric bistable potential $V(x) = 4x^4 + 2x^3 - 8x^2 - 6x$ (see Fig. 1). The potential $V(x)$ has two minima at $x = 1$ and $x = -1$ (metastable state), and a maximum at $x = -\frac{3}{8}$. In Fig. 1, we show the deterministic potential $V(x)$ and the "probabilistic" potential V_{eff} with the corresponding stationary PDFs. Specifically V_{eff} is calculated for $D = 0.32$ and $\mu = 0.45$. A slight shift, due to the term $\ln(g(x))$ in Eq. (13), is present in the position of the extrema both in the potential profiles and corresponding PDFs.

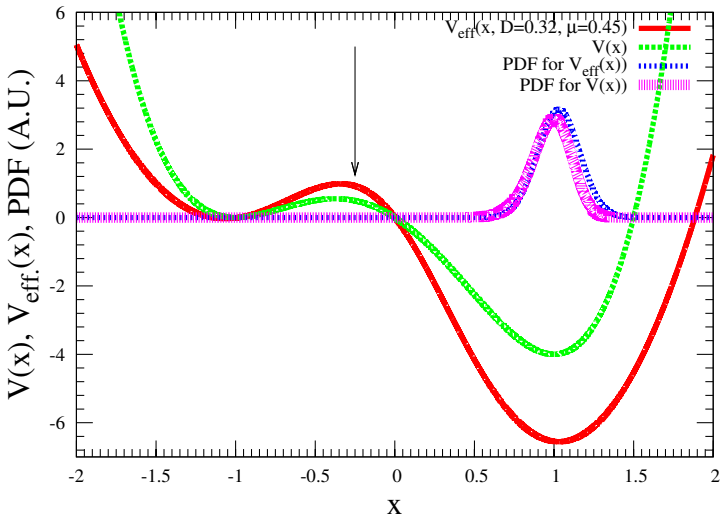

Fig. 1. The deterministic potential $V(x)$ (light grey/green dotted line) and the corresponding PDF (dark grey/magenta dotted line) for the pure additive noise case ($D = 0.32$ and $\mu = 0.0$). The "probabilistic" or effective potential $V_{\text{eff}}(x)$ (continuous black/red line) and the corresponding PDF (black/blue dotted line) in the presence both of multiplicative and additive noise sources ($D = 0.32$ and $\mu = 0.5$). The arrow indicates the initial unstable position of the Brownian particle.

2.2. Mean escape time

By numerical simulation of the Langevin equation

$$dx(t) = \left(-12x^3 - 6x^2 + 16x + 6\right) dt + \sqrt{D + \mu x^2} dW(t)\,, \qquad (14)$$

where $W(t)$ is the Wiener process, we calculate the mean escape time (MET) of the Brownian particle from the metastable state ($x = -1$).

We consider an initial unstable position at $x = -0.25$, just on the right of the maximum (see Fig. 1), and an absorbing barrier at $x = 0.99$. We investigate the MET as a function of two parameters D and μ, by finding a nonmonotonic behavior, with a maximum, of the MET as a function of μ. In Figs. 2, 3 it is shown the behavior of the MET as a function of the

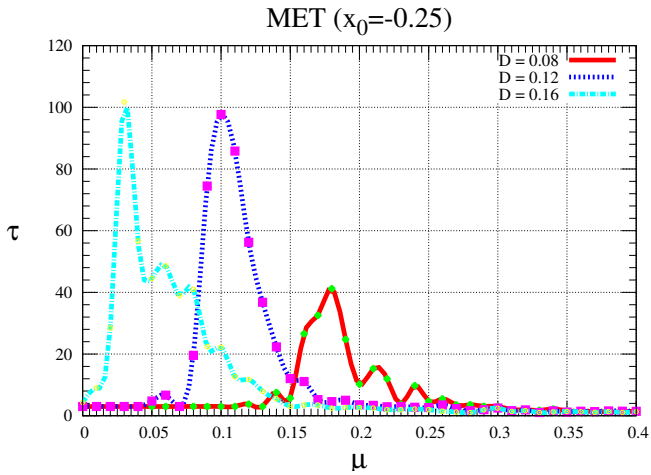

Fig. 2. Plot of the MET as a function of μ for three different values of the parameter D, namely $D = 0.08$ (continuous black/red line), $D = 0.12$ (dark grey/blue dotted line), $D = 0.16$ (light grey/aqua blue dotted line).

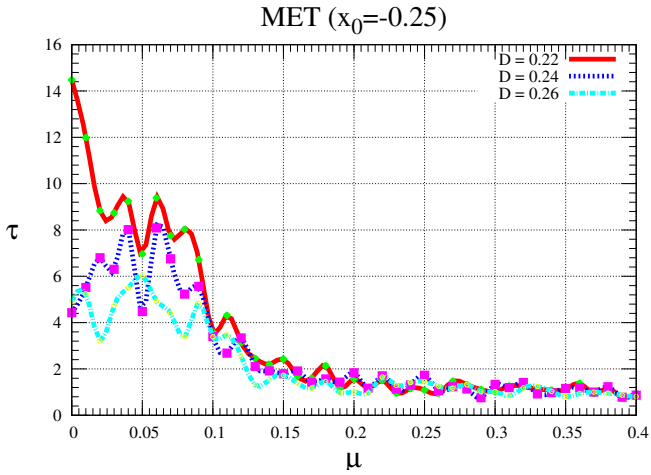

Fig. 3. Plot of the MET as a function of μ for three values of the parameter D, namely $D = 0.22$ (continuous black/red line), $D = 0.24$ (dark grey/blue dotted line), $D = 0.26$ (light grey/aqua blue dotted line).

multiplicative noise intensity μ for six different values of the additive noise intensity D, namely $D = 0.08, 0.12, 0.16, 0.22, 0.24, 0.26$. We observe that for every value of D we have a nonmonotonic trend with a maximum. In particular, for increasing values of D up to ~ 0.18 the maximum of the MET increases, increasing the NES effect, and shift towards low values of the parameter μ. For higher values of D (Fig. 3), the maximum of MET decreases considerably. This means that there is an optimum range of values both of multiplicative and additive noise intensities for which the enhancement of metastability is observed.

3. Cauchy–Lorentz noise effects in the transient dynamics of a short Josephson junction

The dynamics of Josephson junctions (JJ) under the influence of noise signals, namely transient dynamics, constitutes a research topic widely investigated [46–58]. At high temperature, in the thermal activation regime, thermal fluctuations affect the response of the superconductive device in terms of current–voltage characteristic and switching time. The thermal effects can be modeled by a white noise signal applied to the system. When the operating temperatures are low, other noise sources can arise. While thermal noise is originated by the Brownian motion of the charge carriers, nonthermal noise signals are connected with scattering and transmission of the charge carriers. Non-Gaussian noise appears when the conductor, or the superconductor, is in a nonequilibrium state because of the presence of a bias voltage or current. Recently, the dynamics of a JJ in the presence of non-Gaussian noise has been analyzed. The effect of nonthermal noise on the average escape time from the metastable state (superconducting state) of a current-biased JJ, coupled with nonequilibrium current fluctuations, was experimentally investigated [49, 51, 53].

The environmental noise due to thermal or nonthermal noise sources affects significantly the transient dynamics of underdamped and overdamped Josephson junctions. In particular, noise induced effects due to thermal fluctuations, such as resonant activation (RA) and noise enhanced stability (NES), have been theoretically predicted in overdamped JJs [46, 48] and, recently, experimentally revealed in underdamped JJs [7, 59, 60]. Specifically, in Ref. [7] the contemporaneous presence of RA and NES in underdamped JJs has been observed, finding that the average escape times can be enhanced or lowered by using different initial conditions.

In this work, we present a numerical study for the transient dynamics of a short Josephson junction, in the framework of the resistively shunted junction (RSJ) model [61, 62]. In particular, we studied the mean lifetime of the superconductive metastable state of the system, namely the mean

switching time (MST), as a function of the frequency of the driving current signal and the noise intensity. We focused on the simultaneous effects of thermal and non-Gaussian Lévy noise sources. Specifically, a Lévy noise with Cauchy–Lorentz is considered.

3.1. Lévy noise

To investigate the role of non-Gaussian noise, an α-stable distribution is used to generate a non-Gaussian random noise [63]. Lévy processes are characterized by stationary independent increments [64], and its probability distribution belongs to the class of infinitely divisible distributions (i.d.d.) [65, 66]. A subclass of i.d.d. is that of the stable distributions. The general problem of determining the whole class of stable distributions has been solved by Lévy and Khintchine [65]. They obtained the most general expression for the characteristic function of the random stable process [66,67]

$$\varphi(k) = \exp\left[ik\mu - |\sigma k|^{\alpha}\left(1 - i\beta \mathrm{sgn}(k)\Phi\right)\right], \tag{15}$$

where $\mathrm{sgn}(k)$ is the sign function with

$$\begin{cases} \Phi = \tan(\pi\alpha/2), & \text{for all } \alpha \neq 1, \\ \Phi = -(2/\pi)\log|k|, & \text{for } \alpha = 1. \end{cases} \tag{16}$$

Such distributions form a four-parameter family of continuous probability distributions with two shape parameters α and β, a scale parameter σ and a real number μ. Specifically, α $(0 < \alpha \leq 2)$ is the index of stability, β $(\in [-1, 1])$ is an asymmetry parameter, σ is any positive real number which provides for $\alpha = 2$ a measure of the width of the distribution, μ is any real number [67]. The noise intensity of a Lévy distributed noise source is σ^{α}. In Fig. 4, the probability distributions for Gaussian and Cauchy–Lorentz noise, together with the two-dimensional trajectories of free diffusion of a particle in the presence of the same noise sources, are shown.

In comparison with the Gaussian case, Cauchy–Lorentz distribution is narrower in the central part, while at the extremities it goes to zero with less steepness than the Gaussian case (fat tails). The two-dimensional trajectory shown in Fig. 4 (b) and corresponding to the noise signal with Cauchy–Lorentz distribution, presents jumps due to the heavy tails of the distribution. Moreover, the probability to get smaller value is lower than in the Gaussian case and this is evident by comparison of the central part of the Cauchy–Lorentz and Gaussian distributions (see Fig. 4 (a)). This behavior explains the *limited space displacement* of the trajectory corresponding to the Cauchy–Lorentz distribution for relatively low noise intensities (see

Fig. 4 (b)). In other words, the trajectory corresponding to the Cauchy–Lorentz distribution diffuses in space less than the Gaussian one, at short times.

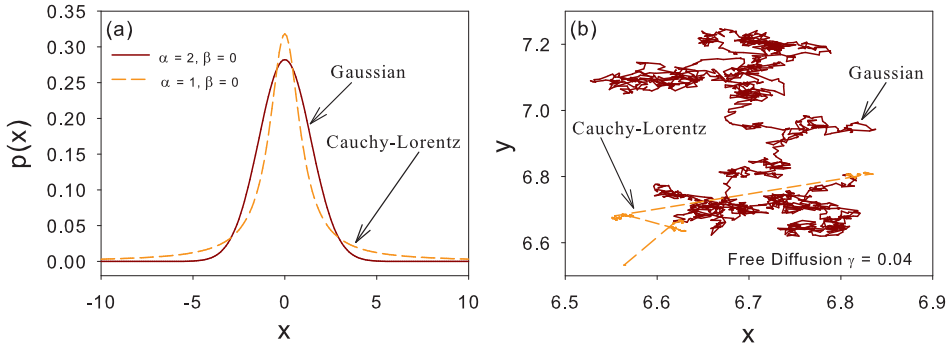

Fig. 4. (a) Probability density function for two stable distributions: Gaussian (solid/dark red line), Cauchy–Lorentz (dashed/orange line). (b) Two-dimensional trajectories of the free diffusion of a particle subjected to noise signals with Gaussian and Cauchy–Lorentz distributions. In both panels, the noise intensity is $\sigma^{\alpha} = 2\gamma$, with $\gamma = 0.04$.

It is worthwhile to note that the large amount of experimental observations of Lévy noise sources in different physical, biological and complex systems determined an increasing interest in the role of non-Gaussian noise in other research fields, such as the transient dynamics of Josephson junctions. Indeed, the Lévy type statistics is observed in various scientific areas, where scale-invariance phenomena take place or can be suspected [68–72] (for a recent review on Lévy-flights see Ref. [71] and references there).

3.2. Simultaneous effects of thermal and non-Gaussian noise

The theoretical description of the dynamics of an overdamped Josephson junction is based on the RSJ model, in which a fictitious Brownian particle is moving in a washboard potential (see Fig. 5). The position of this fictitious particle represents the phase difference φ between the superconducting wave functions on each side of the junction [62]. Nonthermal noise sources could be also present in the system or could be applied externally to it. Therefore, the theoretical investigation of the switching of a JJ, out of its zero voltage state and driven by thermal as well as non-Gaussian noise, will be performed by considering the following Langevin equation for the phase dynamics

$$\frac{d\varphi}{dt} = -\omega_c \frac{dU(\varphi)}{d\varphi} - \omega_c i_{\mathrm{nG}}(t) - \omega_c i_{\mathrm{TN}}(t)\,, \tag{17}$$

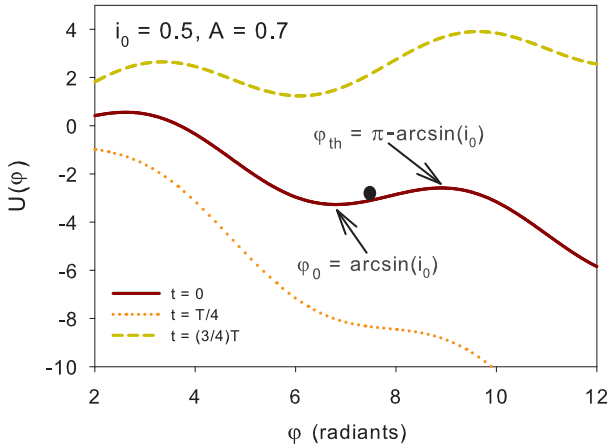

Fig. 5. Washboard Josephson junction potential in the presence of an oscillating driving current. Screen shot of the potential profile at three different instants within one oscillation period T_0: $t = 0$, $t = T_0/4$ and $t = (3/4)T_0$. The arrows indicate the potential minimum located at $\varphi_0 = \arcsin i_0$, corresponding to the initial condition for the fictitious particle (black circle), and the potential maximum at $\varphi_{\rm th} = (\pi - \arcsin i_0)$, corresponding to the threshold position of the particle.

where $i_{\rm TN}(t)$ and $i_{\rm nG}(t)$ are a Gaussian thermal noise and a non-Gaussian noise source, respectively. The $i_{\rm nG}(t)$ has an α-stable distribution with noise intensity σ^α, and α is the Lévy index. The white noise term, $i_{\rm TN}(t)$, is characterized by a zero mean value and an autocorrelation function given by

$$\langle i_{\rm TN}(t) i_{\rm TN}(t')\rangle = \frac{2\gamma_{\rm TN}}{\omega_c}\delta(t-t')\,. \tag{18}$$

The relationship between white current signal and temperature of the system is represented by the dimensionless noise intensity $\gamma_{\rm TN} = 2ek_{\rm B}T/\hbar I_c$, where e is the electron charge, $k_{\rm B}$ the Boltzmann constant, T the temperature, and $\hbar = h/(2\pi)$ with h the Planck constant. The expression of the dimensionless phase potential is

$$U(\varphi) = 1 - \cos(\varphi) + i(t)\varphi\,, \tag{19}$$

where

$$i(t) = i_0 + A\sin\omega t \tag{20}$$

with $i_0(t) = i_b/i_c$ the constant dimensionless bias current, $A\sin\omega t$ the driving current with dimensionless amplitude $A = i_s/i_c$ and frequency ω (i_b and i_s represent the bias current and the driving current amplitude, respectively). The times and frequency will be normalized to the inverse of the characteristic frequency $1/\omega_c$ and to the characteristic frequency ω_c of

the JJ, respectively. In Fig. 5, the potential profile, in the presence of an oscillating driving current, is shown at three different times of the oscillation period T_0.

The minimum of the potential profile, corresponding to $\varphi = \arcsin i_0$, was chosen as the initial position of the particle. The time spent by the particle to reach the next maximum of the potential profile under the influence of the fluctuating potential and noise signal is the first passage time and constitutes the lifetime of the superconductive metastable state. Up to 50,000 realizations of the particle trajectory were obtained, collecting the corresponding first passage times and calculating the mean switching time (MST) of the junction as the average of these times.

In Fig. 6 we show the behavior of the MST in the presence of thermal fluctuations using a non-Gaussian noise source with Cauchy–Lorentz distribution. In particular, we analyse the behavior of MST as a function of the driving signal frequency ω (panel (a)) and the Cauchy–Lorentz noise intensity $\gamma_{\mathrm{Cauchy-Lorentz}}$ (panel (b)), for different values of the thermal noise intensity ($\gamma_{\mathrm{TN}} = 0.0, 0.01, 0.02, 0.1, 0.2, 1, 2$). For zero thermal noise intensity, the corresponding curve of Fig. 6 shows a nonmonotonic behavior with a minimum, which is the signature of the RA phenomenon [19–22,74–78]. We note that the resonant activation effect is a robust enough phenomenon to be observed also in the presence of a Lévy noise source. We observe that the behavior of MST is modified for values of the thermal noise intensity greater than the Cauchy–Lorentz noise intensity $\gamma_{\mathrm{TN}} > \gamma_{\mathrm{Cauchy-Lorentz}} = 0.02$. This modification becomes evident for $\gamma_{\mathrm{TN}} \geq 0.2$. While the position of the minimum is slightly affected by the presence of the thermal noise signal, the METs for low and high frequency values decrease. For very fast fluctuations

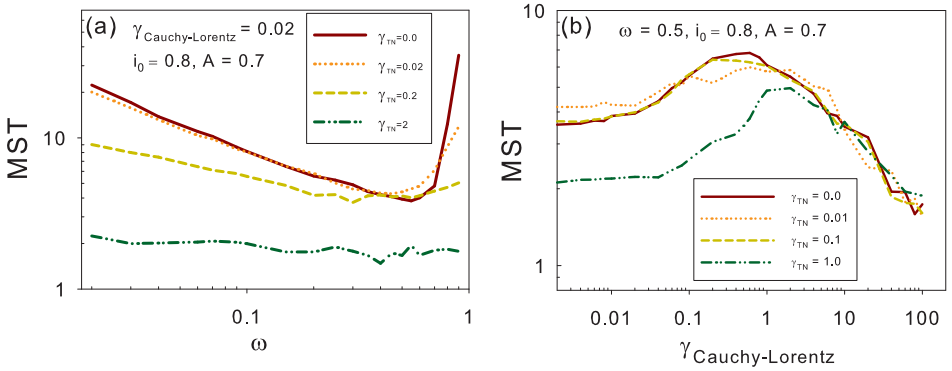

Fig. 6. (a) Log–Log plot of MST *versus* ω for different thermal noise intensities and $\gamma_{\mathrm{Cauchy-Lorentz}} = 0.02$, $i_0 = 0.8$ and $A = 0.7$. (b) MST *versus* $\gamma_{\mathrm{Cauchy-Lorentz}}$ for different thermal noiset intensities and $\omega = 0.5$, $i_0 = 0.8$ and $A = 0.7$.

of the potential profile, the mean escape time is equal to the crossing time over the average barrier *seen* by the Brownian particle. This average barrier coincides with that obtained with the potential profile at $t = 0$ (see Fig. 5) and whose height is $\Delta U = U(\varphi_{\rm th} - U(\varphi_0)) \simeq 2.1$. By using the Kramers formula for the average escape time, we obtain a lower MST by increasing the thermal noise intensity. For very slow oscillations of the potential barrier, the average escape time is equal to the average of the crossing times in the highest and lowest configurations of the barrier, and the slowest escape process determines the value of the average escape time [19]. Again, an increase of the thermal noise intensity produces a decreasing of MST. By further increasing $\gamma_{\rm TN}$, the typical RA behavior of MST *versus* ω disappears because the thermal noise intensity becomes comparable with the height of the potential barrier $\gamma_{\rm TN} \simeq \Delta U(\varphi) \simeq 2$.

In Fig. 6 (b), the MST *versus* $\gamma_{\rm Cauchy-Lorentz}$ is shown. The NES effect is evident in all the curves obtained for different intensities of thermal noise. In the absence of thermal noise ($\gamma_{\rm TN} = 0$), the behavior of the MET as a function of the noise intensity is nonmonotonic with a maximum in correspondence of $\gamma^{\rm max}_{\rm Cauchy-Lorentz} \simeq 0.6$. For thermal noise intensities lower than this value, the NES behavior is unchanged. For greater thermal noise intensities $\gamma_{\rm TN} > 0.6$, the thermal effects are more effective than those due to the Cauchy noise and the nonmonotonic behavior is modified. The maximum of the curve decreases and it is shifted in correspondence to the Cauchy noise intensities of the same order of magnitude of the thermal noise intensities. The simultaneous presence of two noise sources produces an increase of the overall noise intensity "felt" by the system. Moreover, all the curves of MST coalesce together at higher noise intensities, when the structure of the potential profile becomes irrelevant for the dynamics of the particle. The MST has a power-law dependence on the noise intensity [71].

4. Quantum metastable system

Metastability in open quantum systems and relaxation processes from metastable states are a fundamental issue in many branches of physics and chemistry, and recently have been subject of increasing interest [23, 79–87]. In this section, in order to analyze the evolution of a quantum particle, interacting with a thermal bath, initially placed in a metastable state we consider a time-independent asymmetric bistable potential. We use the Caldeira–Leggett model [88] which allows to derive a quantum mechanical analogue of the generalized Langevin equation. The study is performed by using the approach of the Feynman–Vernon functional [89] in *discrete variable representation* (DVR) [23, 90].

4.1. The model

The total Hamiltonian of the system is

$$\hat{H}(t) = \hat{H}_0(t) + \hat{H}_B\,, \tag{21}$$

where

$$\hat{H}_0 = \frac{\hat{p}^2}{2M} + \hat{V}_0(\hat{q}) \tag{22}$$

is the unperturbed Hamiltonian, with $\hat{q}$ and $\hat{p}$ the one-dimensional operators for position and momentum, respectively,

$$\hat{V}_0(\hat{q}) = \frac{M^2\omega_0^4}{64\Delta U}\hat{q}^4 - \frac{M\omega_0^4}{4}\hat{q}^2 - \hat{q}\epsilon \tag{23}$$

is the asymmetric bistable potential shown in Fig. 7, and

$$\hat{H}_B = \sum_{j=1}^{\mathcal{N}} \frac{1}{2}\left[\frac{\hat{p}_j^2}{m_j} + m_j\omega_j^2\left(\hat{x}_j - \frac{c_j}{m_j\omega_j^2}\hat{q}\right)^2\right] \tag{24}$$

is the Hamiltonian which describes the thermal reservoir and its interaction with the particle. In Eq. (23), ϵ and ΔU are the asymmetry parameter and the barrier height, respectively, and ω_0 is the natural oscillation frequency. As usual in the Caldeira–Leggett model, the thermal bath is depicted by an ensemble of $\mathcal{N}$ harmonic oscillators with spatial coordinate $\hat{x}_j$, momentum $\hat{p}_j$, mass m_j, and frequency ω_j. The coefficients c_j are the coupling constant between system and thermal bath. For a reservoir made of harmonic oscillators, we can write the spectral density in a very general way as follows

$$J(\omega) = \frac{\pi}{2}\sum_{j=1}^{N}\frac{c_j}{m_j\omega_j}\delta(\omega - \omega_j)\,, \tag{25}$$

and for $N \longrightarrow \infty$ we obtain a continuous spectral density. In this study, we consider an Ohmic spectral density characterized by an exponential cut-off ω_c as follows

$$J(\omega) = \eta\omega\exp\left(-\frac{\omega}{\omega_c}\right)\,, \tag{26}$$

where $\eta = M\gamma$, γ is the strength of the coupling between system and thermal bath, and η represents the intensity of the environmental noise. Because of the bilinear coupling between the coordinate $\hat{q}$ of the system and the coordinate $\hat{x}$ of the thermal bath, this model is the quantum analogue of a classical system affected by a constant random force [91]. The specific potential profile chosen (see Fig. 7) allows us to study the time evolution

of the quantum particle in a metastable state. We will consider only the 8 lowest energy eigenstates, whose eigenvalues are indicated in the vertical axes of Fig. 7.

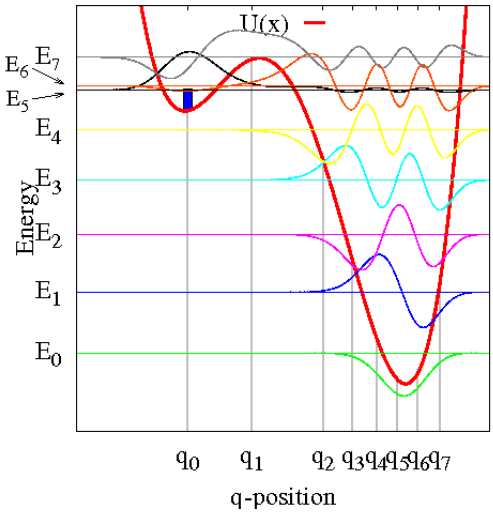

Fig. 7. Potential profile $V_0(q)$ (see Eq. (23)) for $\Delta U = 3$ and $\epsilon = 0.5$. Energy levels and corresponding eigenstates considered in our study are indicated by horizontal lines and curves, respectively. The initial position is $q_{\text{start}} = q_0$ (black/dark blue rectangle). In the horizontal axis are shown the 8 position eigenvalues q_μ ($\mu = 0, \ldots, 7$)

This allows the quantum particle to escape from the metastable states only by tunneling effect. In the same figure, on the horizontal axis the 8 position eigenvalues are shown. The initial position of the particle (black/dark blue rectangle in Fig. 7) coincides with the position eigenvalue q_0 in the metastable state of potential profile. It is worthwhile to note that this position does not coincide with any energy eigenstate, and it is given by a proper linear combination of the 8 energy eigenstates. In the same figure the eigenfunctions corresponding to the 8 energy eigenvalues are also shown.

4.2. The Feynman–Vernon approach

In order to make our analysis independent of the internal degrees of freedom of the thermal bath, we have to trace out the degrees of freedom of the reservoir by using the reduced density operator

$$\rho\left(q_f, q'_f; t\right) = \int dq_0 \int dq'_0 K\left(q_f, q'_f, t; q_0, q'_0, t_0\right) \rho_S\left(q_0, q'_0, t_0\right) , \qquad (27)$$

where the propagator K is given by

$$K\left(q_f, q'_f, t; q_0, q'_0, t_0\right) = \int_{q(t_0)=q_0}^{q(t)=q_f} \mathcal{D}q \int_{q'(t_0)=q'_0}^{q'(t)=q'_f} \mathcal{D}q' \mathcal{A}[q]\mathcal{A}^*[q']\mathcal{F}_{\mathrm{FV}}[q, q'] \tag{28}$$

and

$$\mathcal{A}[q] = \exp\left(i\frac{S_S[q]}{\hbar}\right) \tag{29}$$

with $S_S[q]$ being the classical action functional. In Eq. (28), $\mathcal{F}_{\mathrm{FV}}[q, q'] = \exp\left(-\frac{\phi_{\mathrm{FV}}[q,q']}{\hbar}\right)$ is the Feynman–Vernon influence functional with the influence weight functional $\phi_{\mathrm{FV}}[q, q']$ which is depending on the bath correlation function [91].

4.3. Discrete variable representation

By performing a basis transformation from the energy representation to the so-called *discrete variable representation* (DVR) [23,90], we can describe the localization of the quantum particle. The eigenvalues of the position operator $\hat{q}$ in the basis $\{|q_\mu\rangle\}$ are shown in the horizontal axis of Fig. 7. Within the framework of the DVR, the dynamics of the system, as transitions between energy eigenstates, is transformed in a hopping among the discrete position eigenvalues q_μ. In other words, the dynamics in the DVR basis is described by discrete quantum mechanical paths $q(t)$ which represent a possible temporal evolutions of the system. A complete calculation of these elements in the DVR is given in Ref. [23]. The Eq. (27) contains an infinite sum over all the (infinite) possible paths that the system might follow. In order to calculate the diagonal terms of the density matrix, we have to reduce the number of the levels and the paths taken into account must be only the relevant ones. For this reason, it is necessary to state what kind of approximations we should use. There are several kind of approximations that can be used. For our purposes the more general approximation is the so-called non-interacting cluster approximation. This approximation is valid if the system fulfills the condition

$$\Delta_{\max} = \max\{\Delta_1, \Delta_2, ...\} < \gamma\,, \tag{30}$$

where Δ_j is the energy gap between two neighbor levels. Within this approximation it is possible to derive a master equation which describes the temporal evolution of the system (see Ref. [23,92]).

4.4. Results

We studied the time evolution of our quantum particle taking into account the 8 lowest energy levels (shown in Fig. 7) in order to point out only the contribution to the dynamics of the tunnel effect. It is important to note that the higher energy eigenvalue E_7 has a value which is lower than the value of the maximum of the potential. We analyze the time behavior of the populations for different values of the coupling strength, focusing on the time behavior of the state $|q_0\rangle$, whose position eigenvalue lies in the left side well of the potential. In the DVR-representation, we choose as initial position $q_{\text{start}} = q_0$. By integrating the master equation for a range of values of the parameter η for each eigenstate $|q_\mu\rangle$, the time behavior of the corresponding population $\rho_{q_\mu} \equiv \rho_{\mu\mu}$ (see Fig. 8 and Fig. 9) is obtained. In order

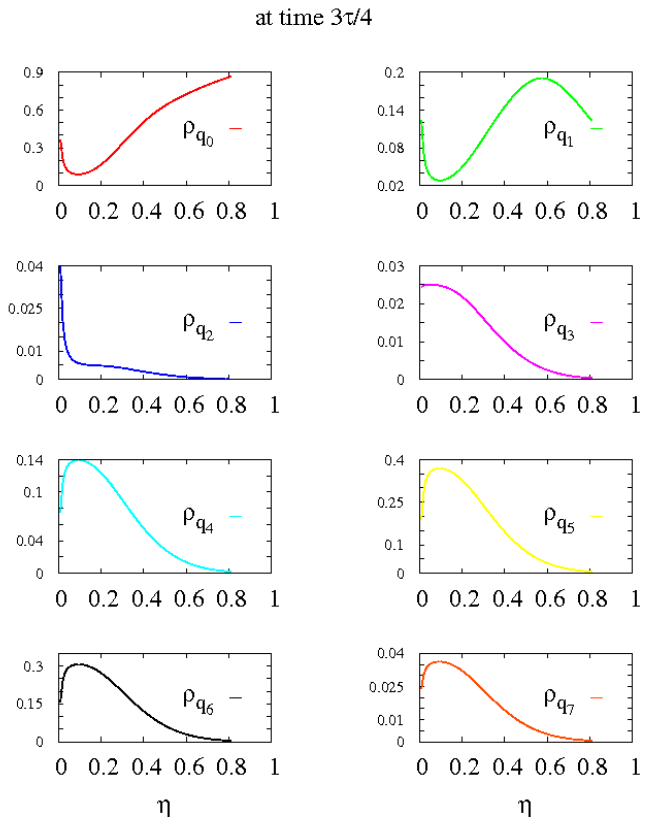

Fig. 8. Behavior of the diagonal elements, ρ_{q_μ} $(\mu = 0, 1, \ldots, 7)$, of the density matrix in q-representation as a function of the noise intensity η at time $t = \frac{3}{4}\tau$. The matrix elements ρ_{q_μ} are the population distributions in the eight position eigenstates considered.

to describe the time evolution of the system for different values of the noise intensity η, we choose as time scale τ the largest of the relaxation times obtained for $\eta = 0.01$ (see Ref. [92] for further details). In Fig. 8 a non-monotonic behavior of the populations as a function of the noise intensity is shown. For the eigenstates $|q_0\rangle$, $|q_1\rangle$ we have a maximum of population at $\eta \simeq 0.1$, while all the other eigenstates have a minimum of population. However, by increasing the noise intensity, the populations corresponding to eigenstates whose position eigenvalues lies in the metastable state increase, and for the q_1 eigenvalue the population reaches a maximum. Finally, as a consequence of the quantum Zeno effect, for $t = 6\tau$ (Fig. 9) and increasing noise intensity η, all populations tend to their initial values, showing the Zeno freezing phenomenon [93].

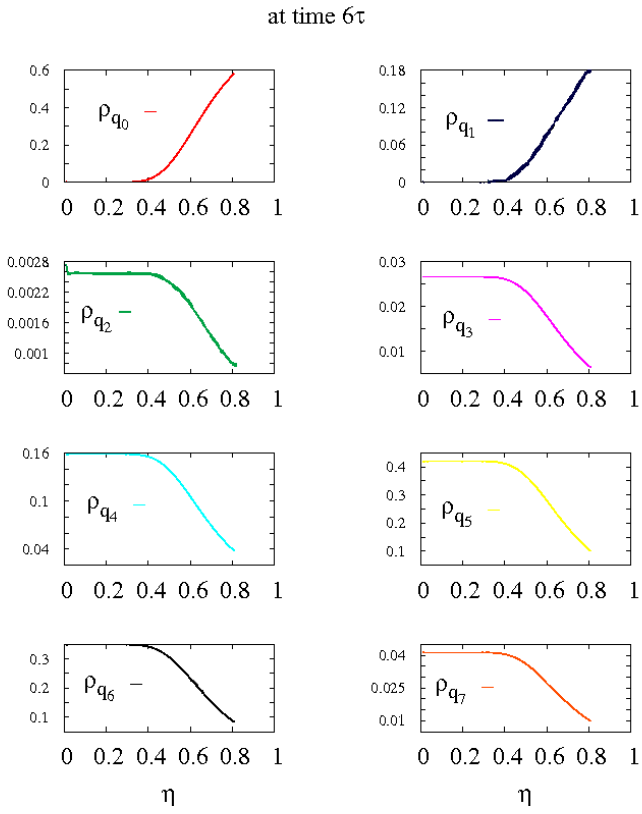

Fig. 9. Behavior of the diagonal elements, ρ_{q_μ} $(\mu = 0, 1, ..., 7)$, of the density matrix in q-representation as a function of the noise intensity η at time $t = 6\tau$. The matrix elements ρ_{q_μ} are the population distributions in the eight position eigenstates considered.

This work was partially supported by MIUR (Ministero dell'Istruzione dell'Universita' e della Ricerca), CNISM (Consorzio Nazionale Interuniversitario per le Scienze Fisiche della Materia) and the Russian Foundation for Basic Research (project 11-02-01418). This work was also partially supported by the EU through Grant No. PITN-GA-2009-234970 and the Joint Italian Japanese Laboratory on "Quantum Technologies" of the Italian Ministry of Foreign Affairs.

REFERENCES

[1] N. Agudov, B. Spagnolo, *Phys. Rev.* **E64**, 035102(R) (2001).
[2] A.A Dubkov, B. Spagnolo, *Phys. Rev.* **E69**, 061103 (2004).
[3] B. Spagnolo, A.A. Dubkov, N.V. Agudov, *Acta Phys. Pol. B* **35**, 1419 (2004).
[4] P. D'Odorico, F. Laio, L. Ridolfi, *Proc. Natl. Acad. Sci. USA* **102**, 10819 (2005).
[5] A. Fiasconaro, B. Spagnolo, S. Boccaletti, *Phys. Rev.* **E72**, 061110 (2005).
[6] P.I. Hurtado, J. Marro, P.L. Garrido, *Phys. Rev.* **E74**, 050101(R) (2006).
[7] G. Sun *et al.*, *Phys. Rev.* **E75**, 021107 (2007).
[8] L. Ridolfi, P. D'Odorico, F. Laio, *J. Theor. Biol.* **248**, 301 (2007).
[9] B. Spagnolo *et al.*, *Acta Phys. Pol. B* **38**, 1925 (2007).
[10] M. Yoshimoto, H. Shirahama, S. Kurosawa, *J. Chem. Phys.* **129**, 014508 (2008).
[11] M. Turcotte, J. Garcia-Ojalvo, G.M. Süel, *Proc. Natl. Acad. Sci. USA* **105**, 15732 (2008).
[12] A. Fiasconaro, B. Spagnolo, *Phys. Rev.* **E80**, 041110 (2009).
[13] M. Trapanese, *J. Appl. Phys.* **105**, 07D313 (2009).
[14] J.H. Li, J. Luczka, *Phys. Rev.* **E82**, 041104 (2010).
[15] A. Fiasconaro, J.J. Mazo, B. Spagnolo, *Phys. Rev.* **E82**, 041120 (2010).
[16] M. Parker, A. Kamenev, B. Meerson, *Phys. Rev. Lett.* **107**, 180603 (2011).
[17] Zheng-Lin Jia, Dong-Cheng Mei, *J. Stat. Mech.: Theory Exp.* **P10010**, (2011).
[18] Dong-Cheng Mei, Zheng-Lin Jia, Can-Jun Wang, *Phys. Scr.* **84**, 045012 (2011).
[19] C.R. Doering, J.C. Gadoua, *Phys. Rev. Lett.* **69**, 2318 (1992).
[20] R.N. Mantegna, B. Spagnolo, *J. Phys. IV France* **8**, 247 (1998).
[21] M. Boguñá, J.M. Porra, J. Masoliver, K. Lindenberg, *Phys. Rev.* **E57**, 3990 (1998).
[22] R.N. Mantegna, B. Spagnolo, *Phys. Rev. Lett.* **84**, 3025 (2000).
[23] M. Thorwart, M. Grifoni, P. Hänggi, *Ann. Phys.* **293**, 15 (2001).
[24] S. Wehner *et al.*, *Phys. Rev. Lett.* **95**, 038301 (2005).

[25] T.S. Biró, A. Jakovác, *Phys. Rev. Lett.* **94**, 132302 (2005).

[26] K.S. Turitsyn, S.A. Derevyanko, I.V. Yurkevich, S.K. Turitsyn, *Phys. Rev. Lett.* **91**, 203901 (2003).

[27] A. Zaikin *et al.*, *Phys. Rev. Lett.* **90**, 030601 (2003).

[28] A.A. Zaikin, J. García-Ojalvo, L. Schimansky-Geier, J. Kurths, *Phys. Rev. Lett.* **88**, 010601 (2001).

[29] F. de Pasquale, J.M. Sancho, M. San Miguel, P. Tartaglia, *Phys. Rev.* **A33**, 4360 (1986).

[30] M.A. Muñoz, in *Advances in Condensed Matter and Statistical Mechanics*, ed. E. Korutcheva, R. Cuerno, Nova Science Publishers, Commack, NY 2003.

[31] L.R. Horsthemke, *Noise-Induced Transitions*, Springer, Berlin 1984.

[32] M.A. Muñoz, F. Colaiori, C. Castellano, *Phys. Rev.* **E72**, 056102 (2005).

[33] O. Chichigina, D. Valenti, B. Spagnolo, *Fluc. Noise Lett.* **5**, L243 (2005).

[34] B. Spagnolo, D. Valenti, A. Fiasconaro, *Math. Biosci. Eng.* **1**, 185 (2004).

[35] D. Valenti, L. Schimansky-Geier, X. Sailer, B. Spagnolo, *Eur. Phys. J.* **B50**, 199 (2006).

[36] B. Spagnolo, A. Fiasconaro, D. Valenti, *Fluc. Noise Lett.* **3**, L177 (2003).

[37] A. Manor, N.M. Shnerb, *Phys. Rev. Lett.* **103**, 030601 (2009).

[38] P. Barrera, S. Ciuchi, B. Spagnolo, *J. Phys. A: Math. Gen.* **26**, L559 (1993).

[39] S. Ciuchi, F. de Pasquale, B. Spagnolo, *Phys. Rev.* **E47**, 3915 (1993).

[40] S. Ciuchi, F. de Pasquale, B. Spagnolo, *Phys. Rev.* **E54**, 706 (1996).

[41] B. Spagnolo, A. La Barbera, *Physica A* **315**, 114 (2002).

[42] P.I. Hurtado, J. Marro, *J. Stat. Phys.* **133**, 29 (2008).

[43] V.I. Klyatskin, *Stochastic Equations Through the Eye of the Physicist*, Elsevier, Amsterdam 2005.

[44] R.L. Stratonovich, *Introduction to the Theory of Random Noise*, Gordon and Breach, New York 1963.

[45] C.W. Gardiner, *Handbook of Stochastic Methods*, Springer-Verlag, Berlin–Heidelberg 1985.

[46] A.L. Pankratov, B. Spagnolo, *Phys. Rev. Lett.* **93**, 177001 (2004).

[47] K.G. Fedorov, A. Pankratov, *Phys. Rev.* **B76**, 024504 (2007).

[48] A.V. Gordeeva, A.L. Pankratov, B. Spagnolo, *Int. J. Bifurcation Chaos* **18**, 2825 (2008).

[49] B. Huard *et al.*, *Ann. Phys.* **16**, 736 (2007).

[50] G. Augello, D. Valenti, B. Spagnolo, *Int. J. Quantum Inf. Suppl.* **6**, 801 (2008).

[51] J.T. Peltonen *et al.*, *Physica E* **40**, 111 (2007).

[52] K.G. Federov, A.L. Pankratov, B. Spagnolo, *Int. J. Bifurcation Chaos* **18**, 2857 (2008).

[53] L. Billings, *Phys. Rev.* **E78**, 051122 (2008).

[54] A.V. Timofeev, dissertation for the degree of Doctor of Science, Helsinki University of Technology, 2009.

[55] G. Augello, D. Valenti, A.L. Pankratov, B. Spagnolo, *Eur. Phys. J.* **B70**, 145 (2009).

[56] T. Novotný, *J. Stat. Mech.: Theory Exp.* **P01050**, (2009).

[57] Q. Le Masne *et al.*, *Phys. Rev. Lett.* **102**, 067002 (2009).

[58] G. Augello, D. Valenti, B. Spagnolo, *Eur. Phys. J.* **B78**, 225 (2010).

[59] Y. Yu, S. Han, *Phys. Rev. Lett.* **91**, 127003 (2003).

[60] C. Pan *et al.*, *Phys. Rev.* **E79**, 030104(R) (2009).

[61] D.E. McCumber, *J. Appl. Phys.* **39**, 3113 (1968).

[62] A. Barone, G. Paternò, *Physics and Application of the Josephson Effect*, Wiley, New York 1982; K.K. Likharev, *Rev. Mod. Phys.* **51**, 101 (1979).

[63] R. Weron, *Stat. Probab. Lett.* **28**, 165 (1996).

[64] K.I. Sato, *Lévy Processes and Infinitely Divisible Distributions*, Cambridge University Press, Cambridge 1999.

[65] A. Khintchine, P. Lévy, *Comptes Rendus* **202**, 374 (1936).

[66] W. Feller, *An Introduction to Probability Theory and Its Applications*, Vol. 2, John Wiley & Sons, Inc., New York 1971.

[67] R.N. Mantegna, H.E. Stanley, *An Introduction to Econophysics. Correlations and Complexity in Finance*, Cambridge University Press, Cambridge 2000.

[68] A.V. Chechkin, V.Yu. Gonchar, J. Klafter, R. Metzler, *Adv. Chem. Phys.* **133**, 439 (2006).

[69] R. Metzler, J. Klafter, *Phys. Rep.* **339**, 1 (2000).

[70] V.V. Uchaikin, *Phys. Usp.* **46**, 821 (2003).

[71] A.A. Dubkov, B. Spagnolo, V.V. Uchaikin, *Int. J. Bifurcation Chaos* **18**, 2649 (2008).

[72] A.A. Dubkov, A. La Cognata, B. Spagnolo, *J. Stat. Mech.: Theory Exp.* **P01002**, (2009).

[73] H. Bergström, *Ark. Mathematicae II* **18**, 375 (1952).

[74] P. Pechukas, P. Hänggi, *Phys. Rev. Lett.* **73**, 2772 (1994).

[75] M. Marchi *et al.*, *Phys. Rev.* **E54**, 3479 (1996).

[76] J. Iwaniszewski, I.K. Kaufman, P.V.E. McClintock, A.J. McKane, *Phys. Rev.* **E61**, 1170 (2000).

[77] B. Dybiec, E. Gudowska-Nowak, *Phys. Rev.* **E66**, 026123 (2002).

[78] B. Dybiec, E. Gudowska-Nowak, *J. Stat. Mech.: Theory Exp.* **P05004**, (2009).

[79] P. Hänggi, P. Talkner, M. Borkovec, *Rev. Mod. Phys.* **62**, 251 (1990).

[80] M. Grifoni, P. Hänggi, *Phys. Rep.* **304**, 229 (1998).

[81] P.K. Ghosh, J.R. Chaudhuri, *J. Stat. Mech.: Theory Exp.* **P02014**, (2008).

[82] V. Peano, M. Thorwart, *Phys. Rev.* **B82**, 155129 (2010).

[83] P. Ghosh, A. Shit, S. Chattopadhyay, J.R. Chaudhuri, *Phys. Rev.* **E82**, 041113 (2010).

[84] S.S. Sinha, A. Ghosh, D.S. Ray, *Phys. Rev.* **E84**, 031118 (2011).

[85] R.A. Kuzyakin, V.V. Sargsyan, G.G. Adamian, N.V. Antonenko, *Phys. Rev.* **A84**, 032117 (2011).

[86] S.S. Sinha, A. Ghosh, D.S. Ray, *Phys. Rev.* **E84**, 041113 (2011).

[87] M.A. Sillanpää, R. Khan, T.T. Heikkilâ, P.J. Hakonen, *Phys. Rev.* **B84**, 195433 (2011).

[88] A.O. Caldeira, A.L. Leggett, *Phys. Rev. Lett.* **46**, 211 (1981).

[89] R.P. Feynman, F.L. Vernon Jr., *Ann. Phys.* **24**, 118 (1963).

[90] D.O. Harris, G.G. Engerholm, W.D. Gwinn, *J. Chem. Phys.* **24**, 1515 (1965).

[91] U. Wiess, *Quantum Dissipative Systems*, World Scientific, Singapore 1999.

[92] P. Caldara *et al.*, *Int. J. Quantum Inf. Suppl.* **9**, 119 (2011).

[93] P. Facchi *et al.*, *Phys. Rev.* **A71**, 022302 (2005).